New parton distribution functions from a global analysis of quantum chromodynamics

Sayipjamal Dulat,[1,2,*] Tie-Jiun Hou,[3,†] Jun Gao,[4,‡] Marco Guzzi,[5,§] Joey Huston,[2,‖] Pavel Nadolsky,[3,¶] Jon Pumplin,[2,**] Carl Schmidt,[2,††] Daniel Stump,[2,‡‡] and C.-P. Yuan[2,§§]

[1]*School of Physics Science and Technology, Xinjiang University, Urumqi, Xinjiang 830046, China*
[2]*Department of Physics and Astronomy, Michigan State University, East Lansing, Michigan 48824, USA*
[3]*Department of Physics, Southern Methodist University, Dallas, Texas 75275-0181, USA*
[4]*High Energy Physics Division, Argonne National Laboratory, Argonne, Illinois 60439, USA*
[5]*School of Physics and Astronomy, University of Manchester, Manchester M13 9PL, United Kingdom*

(Received 6 August 2015; published 16 February 2016)

We present new parton distribution functions (PDFs) at next-to-next-to-leading order (NNLO) from the CTEQ-TEA global analysis of quantum chromodynamics. These differ from previous CT PDFs in several respects, including the use of data from LHC experiments and the new D0 charged-lepton rapidity asymmetry data, as well as the use of a more flexible parametrization of PDFs that, in particular, allows a better fit to different combinations of quark flavors. Predictions for important LHC processes, especially Higgs boson production at 13 TeV, are presented. These CT14 PDFs include a central set and error sets in the Hessian representation. For completeness, we also present the CT14 PDFs determined at the LO and the NLO in QCD. Besides these general-purpose PDF sets, we provide a series of (N)NLO sets with various α_s values and additional sets in general-mass variable flavor number schemes, to deal with heavy partons, with up to three, four, and six active flavors.

DOI: 10.1103/PhysRevD.93.033006

I. INTRODUCTION

Run 1 at the Large Hadron Collider (LHC) was a great success, culminating in the discovery of the Higgs boson [1,2]. No physics beyond the Standard Model was discovered in this run; however, run 2, with a larger center-of-mass energy and integrated luminosity, will allow for an increased discovery potential for new physics. Precision measurements of the Higgs boson and of various electroweak observables will be performed with extraordinary accuracy in new kinematic regimes in run 2. Run-1 achievements, such as the combined ATLAS-CMS measurement of the Higgs boson mass with 0.2% accuracy [3], will soon be superseded. For both precision measurements and for discovery of possible new physics, it is important to have the proper tools for the calculation of the relevant cross sections. These tools include both matrix element determinations at higher orders in perturbative QCD and electroweak theory and precision parton distribution functions (PDFs). The need for precision PDFs was driven home by the recent calculation of the inclusive cross section for gluon-gluon fusion to a Higgs boson at next-to-next-to-next-to-leading order (NNNLO) [4]. As this tour-de-force calculation has significantly reduced the scale dependence of the Higgs cross section, the PDF and α_s uncertainties become the dominant remaining theoretical uncertainty (as of the last PDF4LHC recommendation).

The CT10 parton distribution functions were published at NLO in 2010 [5], followed by the CT10 NNLO parton distribution functions in 2013 [6]. These PDF ensembles were determined using diverse experimental data from fixed-target experiments, HERA and the Tevatron collider, but without data from the LHC. In this paper, we present a next generation of PDFs, designated as CT14. The CT14 PDFs include data from the LHC for the first time, as well as updated data from the Tevatron and from HERA experiments. Various CT14 PDF sets have been produced at the LO, NLO and NNLO and are available from LHAPDF [7].

The CTEQ-TEA philosophy has always been to determine PDFs from data on inclusive, high-momentum transfer processes, for which perturbative QCD is expected to be reliable. For example, in the case of deep-inelastic lepton scattering, we only use data with $Q > 2$ GeV and $W > 3.5$ GeV. Data in this region are expected to be relatively free of nonperturbative effects, such as higher twists or nuclear corrections. Thus, there is no need to introduce phenomenological models for nonperturbative corrections beyond the leading-twist perturbative contributions.

*sdulat@msu.edu
†tiejiunh@mail.smu.edu
‡jgao@anl.gov
§marco.guzzi@manchester.ac.uk
‖huston@pa.msu.edu
¶nadolsky@physics.smu.edu
**pumplin@pa.msu.edu
††schmidt@pa.msu.edu
‡‡stump@pa.msu.edu
§§yuan@pa.msu.edu

cannot be separated. The most important, but not the only, criterion for the selection of PDFs is the minimization of the log-likelihood χ^2 that quantifies agreement of theory and data. In addition, we make some "prior assumptions" about the forms of the PDFs. A PDF set that violates them may be rejected even if it lowers χ^2. For example, we assume that the PDFs are smoothly varying functions of x, without abrupt variations or short-wavelength oscillations. This is consistent with the experimental data and sufficient for making new predictions. No PDF can be negative at the input scale Q_0, to preclude negative cross sections in the predictions. Flavor-dependent ratios or cross section asymmetries must also take physical values, which limits the range of allowed parametrizations in extreme kinematical regions with poor experimental constraints. For example, in the CT14 parametrization we restricted the functional forms of the u and d PDFs so that $d(x,Q_0)/u(x,Q_0)$ would remain finite and nonzero at $x \to 1$; cf. the Appendix. We now review every input of the CT14 PDF analysis in turn, starting with the selection of the new experiments.

B. Selection of experiments

The experimental data sets that are included in the CT14 global analysis are listed in Tables I (lepton scattering) and II (production of inclusive lepton pairs and jets). There are a total of 2947 data points included from 33 experiments, producing a χ^2 value of 3252 for the best fit (with $\chi^2/N_{pt} = 1.10$). It can be seen from the values of χ^2 in Tables I and II that the data and theory are in reasonable agreement for most experiments. The variable S_n in the last column is an "effective Gaussian variable," first introduced in Sec. V of Ref. [5] and defined for the current analysis in Refs. [6,22]. The effective Gaussian variable quantifies compatibility of any given data set with a particular PDF fit in a way that is independent of the number of points $N_{pt,n}$ in the data set. It maps the χ^2_n values of individual experiments, whose probability distributions depend on $N_{pt,n}$ in each experiment (and thus, are not identical), onto S_n values that obey a cumulative probability distribution shared by all experiments, independently of $N_{pt,n}$. Values of S_n between -1 and $+1$ correspond to a good fit to the nth experiment (at the 68% C.L.). Large positive values ($\gtrsim 2$) correspond to a poor fit, while large negative values ($\lesssim -2$) are fit unusually well.

The goodness of fit for CT14 NNLO is comparable to that of our earlier PDFs, but the more flexible parametrizations did result in improved agreement with some data sets. For example, by adding additional parameters to the $\{u, \overline{u}\}$ and $\{d, \overline{d}\}$ parton distributions, somewhat better agreement was obtained for the BCDMS and NMC data at low values of Q. The quality of the fit can be also evaluated based on the distribution of S_n values, which follows a standard normal distribution (of width 1) in an ideal fit. As in the previous fits, the actual S_n distribution (cf. the solid curve in Fig. 1) is somewhat wider than the standard normal one (the dashed curve), indicating the presence of disagreements, or tensions, between some of the included experiments. The tensions have been examined before [5,51–53] and originate largely from experimental issues, almost independent of the perturbative QCD order or PDF parametrization form. A more detailed discussion of the level of agreement between data and theory will be provided in Sec. IV.

1. Experimental data from the LHC

Much of these data have also been used in previous CT analyses, such as the one that produced the CT10 NNLO PDFs. As mentioned, no LHC data were used in the CT10

TABLE I. Experimental data sets employed in the CT14 analysis. These are the lepton deep-inelastic scattering experiments. $N_{pt,n}, \chi^2_n$ are the number of points and the value of χ^2 for the nth experiment at the global minimum. S_n is the effective Gaussian parameter [5,6,22] quantifying agreement with each experiment.

ID No.	Experimental data set		$N_{pt,n}$	χ^2_n	$\chi^2_n/N_{pt,n}$	S_n
101	BCDMS F_2^p	[23]	337	384	1.14	1.74
102	BCDMS F_2^d	[24]	250	294	1.18	1.89
104	NMC F_2^d/F_2^p	[25]	123	133	1.08	0.68
106	NMC $\sigma^p_{\rm red}$	[25]	201	372	1.85	6.89
108	CDHSW F_2^p	[26]	85	72	0.85	−0.99
109	CDHSW F_3^p	[26]	96	80	0.83	−1.18
110	CCFR F_2^p	[27]	69	70	1.02	0.15
111	CCFR xF_3^p	[28]	86	31	0.36	−5.73
124	NuTeV $\nu\mu\mu$ semi-inclusive DIS	[29]	38	24	0.62	−1.83
125	NuTeV $\bar{\nu}\mu\mu$ semi-inclusive DIS	[29]	33	39	1.18	0.78
126	CCFR $\nu\mu\mu$ semi-inclusive DIS	[30]	40	29	0.72	−1.32
127	CCFR $\bar{\nu}\mu\mu$ semi-inclusive DIS	[30]	38	20	0.53	−2.46
145	H1 σ_r^b	[31]	10	6.8	0.68	−0.67
147	Combined HERA charm production	[32]	47	59	1.26	1.22
159	HERA1 combined DIS	[33]	579	591	1.02	0.37
169	H1 F_L	[34]	9	17	1.92	1.7

TABLE II. The same as Table I, showing experimental data sets on Drell-Yan processes and inclusive jet production.

ID No.	Experimental data set		$N_{pt,n}$	χ^2_n	$\chi^2_n/N_{pt,n}$	S_n
201	E605 Drell-Yan process	[35]	119	116	0.98	−0.15
203	E866 Drell-Yan process, $\sigma_{pd}/(2\sigma_{pp})$	[36]	15	13	0.87	−0.25
204	E866 Drell-Yan process, $Q^3 d^2\sigma_{pp}/(dQdx_F)$	[37]	184	252	1.37	3.19
225	CDF run-1 electron A_{ch}, $p_{T\ell} > 25$ GeV	[38]	11	8.9	0.81	−0.32
227	CDF run-2 electron A_{ch}, $p_{T\ell} > 25$ GeV	[39]	11	14	1.24	0.67
234	D0 run-2 muon A_{ch}, $p_{T\ell} > 20$ GeV	[40]	9	8.3	0.92	−0.02
240	LHCb 7 TeV 35 pb^{-1} W/Z $d\sigma/dy_\ell$	[41]	14	9.9	0.71	−0.73
241	LHCb 7 TeV 35 pb^{-1} A_{ch}, $p_{T\ell} > 20$ GeV	[41]	5	5.3	1.06	0.30
260	D0 run-2 Z rapidity	[42]	28	17	0.59	−1.71
261	CDF run-2 Z rapidity	[43]	29	48	1.64	2.13
266	CMS 7 TeV 4.7 fb^{-1}, muon A_{ch}, $p_{T\ell} > 35$ GeV	[44]	11	12.1	1.10	0.37
267	CMS 7 TeV 840 pb^{-1}, electron A_{ch}, $p_{T\ell} > 35$ GeV	[45]	11	10.1	0.92	−0.06
268	ATLAS 7 TeV 35 pb^{-1} W/Z cross sec., A_{ch}	[46]	41	51	1.25	1.11
281	D0 run-2 9.7 fb^{-1} electron A_{ch}, $p_{T\ell} > 25$ GeV	[14]	13	35	2.67	3.11
504	CDF run-2 inclusive jet production	[47]	72	105	1.45	2.45
514	D0 run-2 inclusive jet production	[48]	110	120	1.09	0.67
535	ATLAS 7 TeV 35 pb^{-1} incl. jet production	[49]	90	50	0.55	−3.59
538	CMS 7 TeV 5 fb^{-1} incl. jet production	[50]	133	177	1.33	2.51

fits. Nonetheless, the CT10 PDFs have been in good agreement with LHC measurements so far.

As the quantity of the LHC data has increased, the time has come to include the most germane LHC measurements into CT fits. The LHC has measured a variety of Standard Model cross sections, yet not all of them are suitable for determination of PDFs according to the CT method. For that, we need to select measurements that are experimentally and theoretically clean and are compatible with the global set of non-LHC hadronic experiments.

In the CT14 study, we select a few such LHC data sets at $\sqrt{s} = 7$ TeV, focusing on the measurements that provide novel information to complement the non-LHC data. From vector boson production processes, we selected W/Z cross sections and the charged-lepton asymmetry measurement from ATLAS [46], the charged-lepton asymmetry in the electron [45] and muon decay channels [44] from CMS, and the W/Z lepton rapidity distributions and charged-lepton asymmetry from LHCb [41]. The ATLAS and CMS measurements primarily impose constraints on the light quark and antiquark PDFs at $x \gtrsim 0.01$. The LHCb data sets, while statistically limited, impose minor constraints on $\overline{u}$ and d PDFs at $x = 0.05$–0.1.

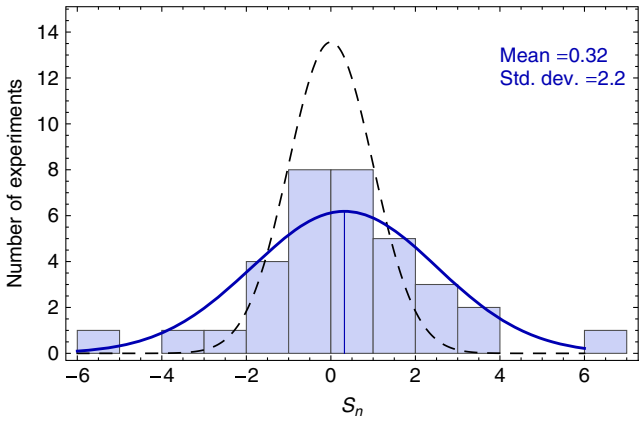

FIG. 1. Best-fit S_n values of 33 experiments in the CT14 analysis.

Upon including these measurements, we can relax the parametric constraints on the sea (anti)quark PDFs of u, $\overline{u}$, d, and $\overline{d}$. In the absence of relevant experimental constraints in the pre-CT14 fits, the PDF parametrizations were chosen so as to enforce $\overline{u}/\overline{d} \to 1$, $u/d \to 1$ at $x \to 0$ in order to obtain convergent fits. As reviewed in the Appendix, the CT14 parametrization form is more flexible, in the sense that only the asymptotic power x^{a_1} is required to be the same in all light-quark PDFs in the $x \to 0$ limit. This choice produces wider uncertainty bands on u_v, d_v, and $\overline{u}/\overline{d}$ at $x \to 0$, with the spread constrained by the newly included LHC data.

From the other LHC measurements, we now include single-inclusive jet production at ATLAS [49] and CMS [50]. These data sets provide complementary information to Tevatron inclusive jet production cross sections from CDF run 2 [47] and D0 run 2 [48] that are also included. The purpose of jet production cross sections is primarily to constrain the gluon PDF $g(x, Q)$. While the uncertainties from the LHC jet cross sections are still quite large, they probe the gluon PDF across a much wider range of x than the Tevatron jet cross sections.

One way to gauge the sensitivity of a specific data point to some PDF $f(x, Q)$ at a given x and Q is to compute a correlation cosine between the theoretical prediction for this point and $f(x, Q)$ [13,15,54]. In the case of CT10 NNLO, the sensitivity of the LHC charge asymmetry data

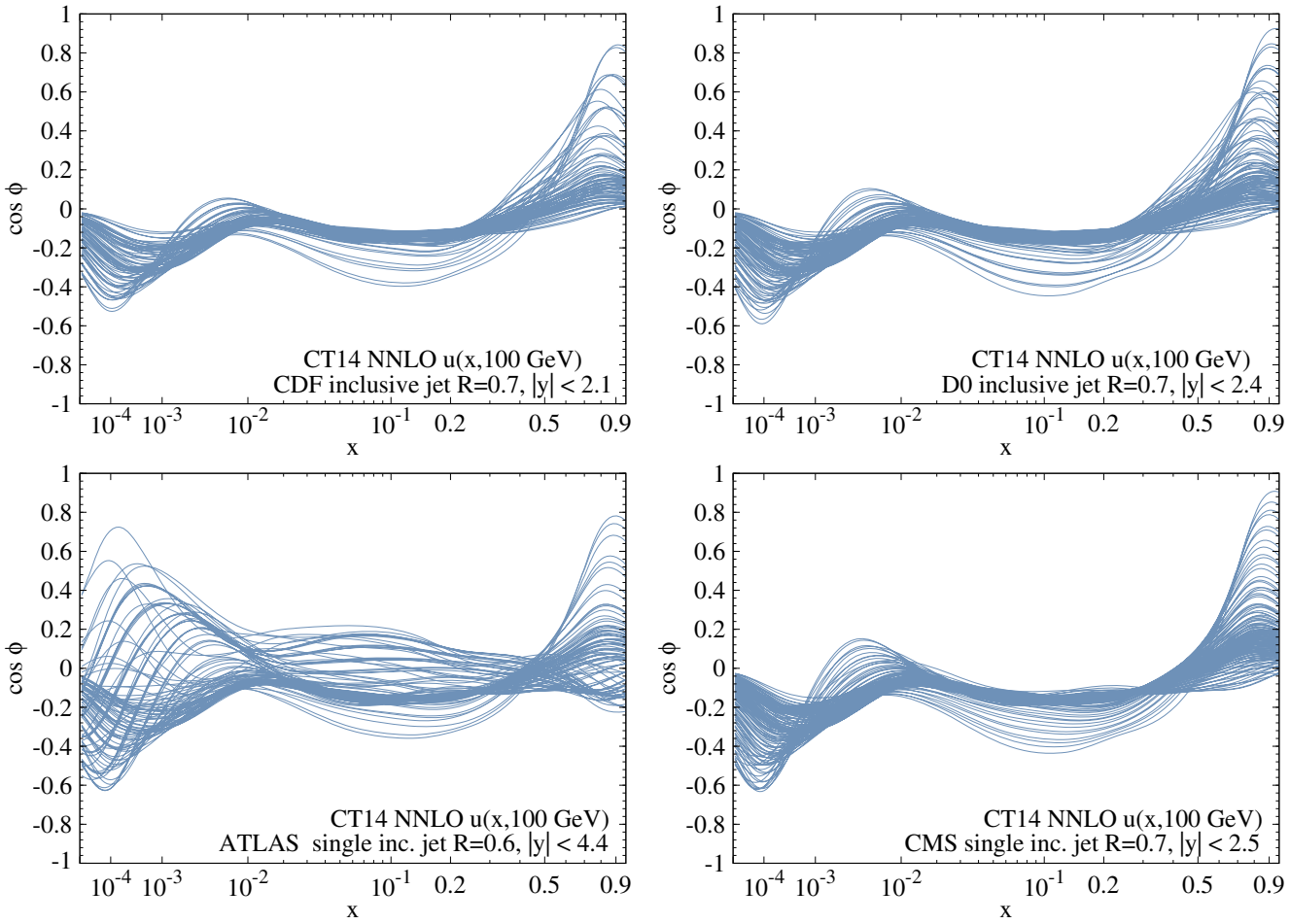

FIG. 4. The correlation cosine $\cos\phi$ [13] between the u-PDF at the specified x value on the horizontal axis and NLO predictions for the CDF [47] (upper left panel), D0 [48] (upper right panel), ATLAS [49] (lower left panel) and CMS [50] (lower right panel) inclusive jet cross sections at $Q = 100$ GeV.

For the ATLAS [49], CMS [50], CDF [47] and D0 [48] inclusive jet data sets, the correlation cosine, $\cos\phi$, for gluon PDF is plotted in Fig. 3 using NLO QCD theory to evaluate the theoretical cross section. Again, the lines correspond to individual p_{Tj} bins of the data. We observe that the CDF and D0 jet cross sections are highly correlated with the gluon PDF $g(x, Q)$ at $x \gtrsim 0.05$ and anticorrelated at small x as a consequence of the momentum sum rule. The ATLAS and CMS jet cross sections are highly correlated with $g(x, Q)$ in a much wider range, $x > 0.005$. In contrast, the PDF-induced correlation of the jet cross sections with the quark PDFs, such as $u(x, Q)$ in Fig. 4, is at most moderate. The ATLAS and CMS jet data therefore have the potential to reduce the gluon uncertainty, but significant reduction will require the data from run 2.

2. High-luminosity lepton charge asymmetry from the Tevatron

Forward-backward asymmetry (A_{ch}) distributions of charged leptons from inclusive weak boson production at the Tevatron are uniquely sensitive to the average slope of the ratio $d(x, Q)/u(x, Q)$ at large x, of order 0.1 and above. In the CT14 analysis, we include several data sets of A_{ch} measured at $\sqrt{s} = 1.8$ and 1.96 TeV by the CDF and D0 Collaborations. The CDF run-1 data set on A_{ch} [38,55], which was instrumental in resolving conflicting information on the large-x behavior of $u(x, Q)$ and $d(x, Q)$ from contemporary fixed-target DIS experiments [56–59], is supplemented by the CDF run-2 data set at 170 pb^{-1} [39]. A_{ch} data at $\sqrt{s} = 1.96$ TeV from D0 in the electron [14] and muon [40] decay channels, for 9.7 and 0.3 fb^{-1}, are also included. In all A_{ch} data sets, we include subsamples with the cuts on the transverse momentum $p_{T\ell}$ of the final-state lepton specified in Table II.

The electron data set (9.7 fb^{-1}) from D0 that we now include replaces the 0.75 fb^{-1} counterpart set [21], first included in CT10. This replacement has an important impact on the determination of the large-x quark PDFs; thus, these new A_{ch} data sets are perhaps the most challenging and valuable among all that were added in CT14.

The D0 A_{ch} data have small experimental errors and hence push the limits of the available theoretical

calculations. Relatively small differences in the average slope (with respect to x) of the d/u ratio in the probed region can produce large variations in χ^2_n for the Tevatron charge asymmetry [56–58]. By varying the minimal selection cuts on $p_{T\ell}$ of the lepton, it is possible to probe subtle features of the large-x PDFs. For that, understanding of the transverse momentum dependence in both experiment and theory is necessary, which demands evaluation of transverse momentum resummation effects.

When the first Tevatron run-2 A_{ch} data sets were implemented in CT fits, significant tensions were discovered between the electron and muon channels, and even between different $p_{T\ell}$ bins within one decay channel. The tensions prompted a detailed study in the CT10 analysis [5]. The study found that various $p_{T\ell}$ bins of the electron and muon asymmetries from D0 disagree with DIS experiments and among themselves.

In light of these unresolved tensions, we published a CT10 PDF ensemble at NLO, which did not include the D0 run-2 A_{ch} data and yielded a d/u ratio that was close to that ratio in CTEQ6.6 NLO. An alternative CT10W NLO ensemble was also constructed. It included four $p_{T\ell}$ bins of that data and predicted a harder d/u behavior at $x \to 1$. When constructing the counterpart CT10 NNLO PDFs in [6], we took an in-between path and included only the two most inclusive $p_{T\ell}$ bins, one from the electron [21] and one from the muon [40] samples. This choice still resulted in a larger d/u asymptotic value in CT10 NNLO than in CTEQ6.6.

The new A_{ch} data for 9.7 fb^{-1} in the electron channel are more compatible with the other global fit in the data that we included. Therefore, CT14 includes the D0 A_{ch} measurement in the muon channel with $p_{T\ell} > 20$ GeV [40] and in the electron channel with $p_{T\ell} > 25$ GeV [14]. The replacement does not affect the general behavior of the PDFs, except that the CT14 d/u ratio at high x follows the trends of CTEQ6.6 NLO and CT10 NLO, rather than of CT10W NLO and CT10 NNLO.

3. New HERA data

CT14 includes a combined HERA-1 data set of reduced cross sections for semi-inclusive DIS production of open charm [32] and measurements of the longitudinal structure function $F_L(x, Q)$ in neutral-current DIS [34]. The former replaces independent data sets of charm structure functions and reduced cross sections from H1 and ZEUS [60–63]. Using the combined HERA charm data set, we obtain a slightly smaller uncertainty on the gluon at $x < 0.01$ and better constraints on charm mass than with independent sets [64]. The latter HERA data set, on F_L, is not independent from the combined HERA set on inclusive DIS [33] but has only nine data points and does not significantly change the global χ^2. Its utility is primarily to prevent unphysical solutions for the gluon PDF at small x at the stage of the PDF error analysis.

4. Other LHC results

One class of LHC data that could potentially play a large role [13] in the determination of the gluon distribution, especially at high x, is the differential distributions of $t\bar{t}$ production, now available from ATLAS [65] and CMS [66,67]. However, these data are not included into our fit, as the differential NNLO $t\bar{t}$ cross section predictions for the LHC are not yet complete and the total cross section measurements lack statistical power. [68]. In addition, constraints on the PDFs from $t\bar{t}$ cross sections are mutually correlated with the values of QCD coupling and top-quark mass. NLO electroweak corrections, playing an important role [69,70] for these data, are still unavailable for some $t\bar{t}$ kinematic distributions. Once these calculations are completed, they will be incorporated in future versions of CT PDFs. For now, we simply show predictions from CT14 for the $t\bar{t}$ distributions using the approximate NNLO calculations in Sec. V.

C. Summary of theoretical calculations

1. QCD cross sections

The CT14 global analysis prioritizes the selection of published data for which NNLO predictions are available, and theoretical uncertainties of various kinds are well understood. Theoretical calculations for neutral-current DIS are based on the NNLO implementation [8] of the SACOT-χ factorization scheme [9–11] with massive quarks. For inclusive distributions in the low-mass Drell-Yan process, NNLO predictions are obtained with the program VRAP [71,72]. Predictions for W/Z production and weak boson charge asymmetries with $p_{T\ell}$ cuts are obtained with the NNLL-(approximately NNLO) program ResBos [73–76], as in the previous analyses.

As already mentioned in the introduction, two exceptions from this general rule concern charged-current DIS and collider jet production. Both have unique sensitivities to crucial PDF combinations but are still known only to NLO. The CCFR and NuTeV data on inclusive and semi-inclusive charge-current DIS are indispensable for constraining the strangeness PDF; single-inclusive jet production at the Tevatron and now at the LHC are essential for constraining the gluon distribution. Yet, in both categories, the experimental uncertainties are fairly large and arguably diminish the impact of missing NNLO effects. Given the importance of these measurements, our approach is then to include these data in our NNLO global PDF fits but evaluate their matrix elements at NLO.

According to this choice, we do not rely on the use of threshold resummation techniques [77,78] to approximate the NNLO corrections in jet production. Nor do we remove the LHC jet data due to the kinematic limitations of such resummation techniques [79]. A large effort was invested in the CT10 and CT14 analyses to estimate the possibility of biases in the NNLO PDFs due to using NLO cross sections

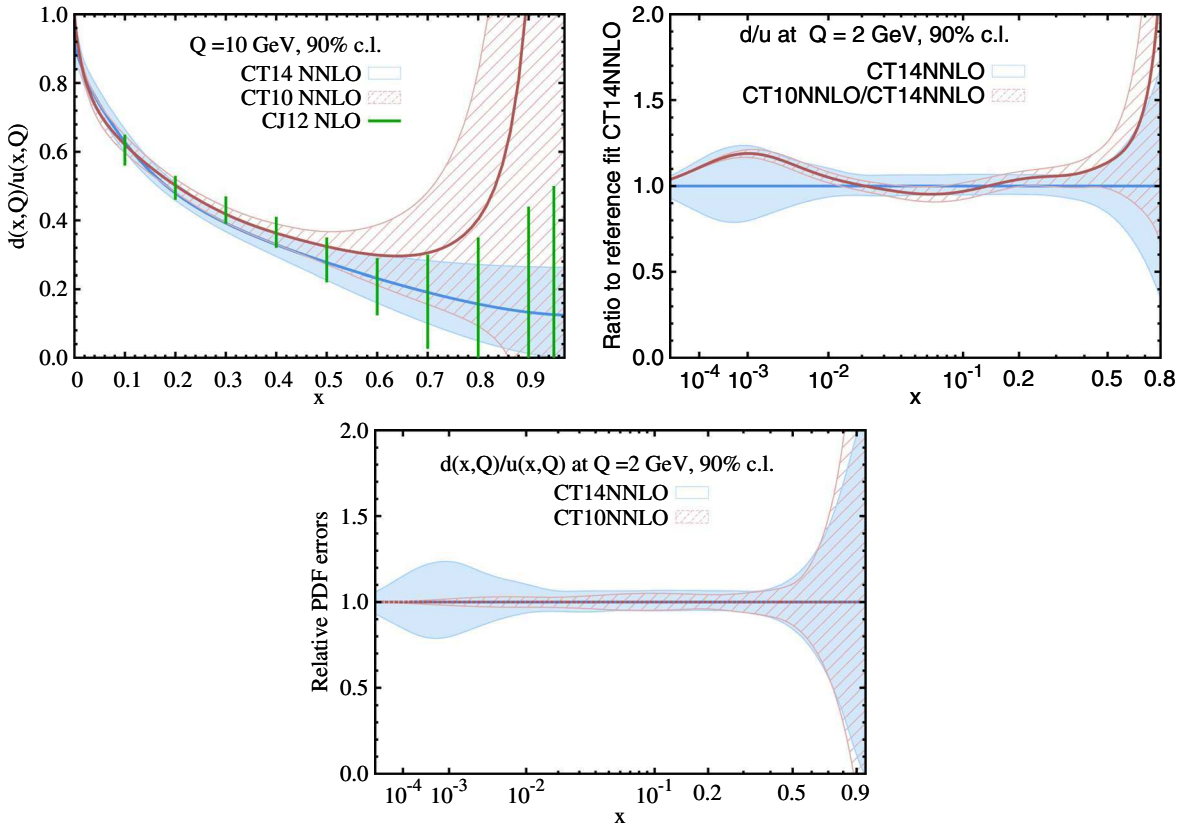

FIG. 7. A comparison of 90% C.L. uncertainties on the ratio $d(x,Q)/u(x,Q)$ for CT14 NNLO (solid blue) and CT10 NNLO (dashed red), and CJ12 NLO (green lines) error ensembles.

relative PDF uncertainties remain about the same. This can be better seen from a direct comparison of the relative PDF uncertainties (normalized to their respective central PDFs) in the third inset. The collider charge asymmetry data constrain d/u at x up to about 0.4. At even higher x, outside of the experimental reach, the behavior of the CT14 PDFs reflects the parametrization form, which now allows d/u to approach any constant value at $x \to 1$.

At such high x, the CTEQ-JLab analysis (CJ12) [94] has independently determined the ratio d/u at NLO, by including the fixed-target DIS data at lower W and higher x that are excluded by a selection cut $W > 3.5$ GeV in CT14 and by considering higher-twist and nuclear effects that can be neglected in the kinematic range of CT14 data. The CT14 uncertainty band on d/u at NNLO lies for the most part between the CJmin and CJmax predictions at NLO that demarcate the CJ12 uncertainty; cf. the first inset of Fig. 7. We see that the CT14 predictions on d/u at $x > 0.1$, which were derived from high-energy measurements that are not affected by nuclear effects, fall within the CJ12 uncertainty range obtained from low-energy DIS with an estimate of various effects beyond leading-twist perturbative QCD. The ratio should be stable to inclusion of NNLO effects; thus, the two ensembles predict a similar trend for collider observables sensitive to d/u.

Turning now to the ratios of sea quark PDFs in Fig. 8, we observe that the uncertainty on $\overline{d}(x,Q)/\overline{u}(x,Q)$ in the left inset has also increased at small x in CT14 NNLO. At $x > 0.1$, we assume that both $\overline{u}(x,Q_0)$ and $\overline{d}(x,Q_0)$ are proportional to $(1-x)^{a_2}$ with the same power a_2; the ratio $\overline{d}(x,Q_0)/\overline{u}(x,Q_0)$ can thus approach a constant value that comes out to be close to 1 in the central fit, while the parametrization in CT10 forced it to vanish. The uncertainty on $\overline{d}/\overline{u}$ has also increased across most of the x range.

The overall reduction in the strangeness PDF at $x > 0.01$ leads to a smaller ratio of the strange-to-nonstrange sea quark PDFs, $(s(x,Q)+\overline{s}(x,Q))/(\overline{u}(x,Q)+\overline{d}(x,Q))$, presented in the right inset of Fig. 8. At $x < 0.01$, this ratio is determined entirely by parametrization form and was found in CT10 to be consistent with the exact $SU(3)$ symmetry of PDF flavors, $(s(x,Q)+\overline{s}(x,Q))/(\overline{u}(x,Q)+\overline{d}(x,Q)) \to 1$ at $x \to 0$, albeit with a large uncertainty. The $SU(3)$-symmetric asymptotic solution at $x \to 0$ is still allowed in CT14 as a possibility, even though the asymptotic limit of the central CT14 NNLO has been reduced and is now at about 0.6 at $x = 10^{-5}$. The uncertainty of strangeness has increased at such small x and now allows $(s(x,Q)+\overline{s}(x,Q))/(\overline{u}(x,Q)+\overline{d}(x,Q))$ between 0.35 and 2.5 at $x = 10^{-5}$.

were obtained using the Lagrange multiplier method: one with enhanced gluon and one with suppressed gluon at small x, as was already done in CT10. In CT14, we also include an additional pair of sets with enhanced or suppressed strangeness at small x; although it is possible that treating $a_1(s)$ as a fitting parameter independent from $a_1(\overline{u}) = a_1(\overline{d})$ would have worked equally well.

In summary, we have a total of 56 error sets: 2×26 from the Hessian method, supplemented by two extremes of small-x gluon, and two extremes of small-x strangeness. Uncertainties from all pairs of error sets are to be summed in quadrature using the master formulas [5,20,54]. In comparison, CT10 NNLO had 50 error sets. The increased flexibility in the CT14 parametrization is warranted by better experimental constraints and its improved fit to the data. Indeed, fitting the CT14 data set using the old CT10 parametrizations yields a best fit that is worse by 60 units in χ^2.

[1] ATLAS Collaboration, Phys. Lett. B **716**, 1 (2012).
[2] CMS Collaboration, Phys. Lett. B **716**, 30 (2012).
[3] ATLAS Collaboration and CMS Collaboration, Phys. Rev. Lett. **114**, 191803 (2015).
[4] C. Anastasiou, C. Duhr, F. Dulat, F. Herzog, and B. Mistlberger, Phys. Rev. Lett. **114**, 212001 (2015).
[5] H.-L. Lai, M. Guzzi, J. Huston, Z. Li, P. M. Nadolsky, J. Pumplin, and C.-P. Yuan, Phys. Rev. D **82**, 074024 (2010).
[6] J. Gao, M. Guzzi, J. Huston, H.-L. Lai, Z. Li, P. Nadolsky, J. Pumplin, and D. Stump, and C.-P. Yuan, Phys. Rev. D **89**, 033009 (2014).
[7] https://lhapdf.hepforge.org/.
[8] M. Guzzi, P. M. Nadolsky, H.-L. Lai, and C.-P. Yuan, Phys. Rev. D **86**, 053005 (2012).
[9] M. A. G. Aivazis, J. C. Collins, F. I. Olness, and W.-K. Tung, Phys. Rev. D **50**, 3102 (1994).
[10] J. C. Collins, Phys. Rev. D **58**, 094002 (1998).
[11] W.-K. Tung, S. Kretzer, and C. Schmidt, J. Phys. G **28**, 983 (2002).
[12] W.-K. Tung, H.-L. Lai, A. Belyaev, J. Pumplin, D. Stump, and C.-P. Yuan, J. High Energy Phys. 02 (2007) 053.
[13] P. M. Nadolsky, H.-L. Lai, Q. H. Cao, J. Huston, J. Pumplin, D. Stump, W.-K. Tung, and C.-P. Yuan, Phys. Rev. D **78**, 013004 (2008).
[14] V. M. Abazov *et al.* (D0 Collaboration), Phys. Rev. D **91**, 032007 (2015); **91**, 079901(E) (2015).
[15] J. Pumplin, D. Stump, R. Brock, D. Casey, J. Huston, J. Kalk, H.-L. Lai, and W.-K. Tung, Phys. Rev. D **65**, 014013 (2001).
[16] G. Watt and R. S. Thorne, J. High Energy Phys. 08 (2012) 052.
[17] D. Stump, J. Pumplin, R. Brock, D. Casey, J. Huston, J. Kalk, H.-L. Lai, and W.-K. Tung, Phys. Rev. D **65**, 014012 (2001).
[18] K. A. Olive *et al.* (Particle Data Group Collaboration), Chin. Phys. C **38**, 090001 (2014).
[19] S. Alekhin *et al.*, arXiv:1101.0536.
[20] J. Pumplin, D. R. Stump, J. Huston, H.-L. Lai, P. M. Nadolsky, and W.-K. Tung, J. High Energy Phys. 07 (2002) 012.
[21] V. Abazov *et al.* (D0 Collaboration), Phys. Rev. Lett. **101**, 211801 (2008).
[22] S. Dulat, T.-J. Hou, J. Gao, J. Huston, J. Pumplin, C. Schmidt, D. Stump, and C.-P. Yuan, Phys. Rev. D **89**, 073004 (2014).
[23] A. C. Benvenuti *et al.* (BCDMS Collaboration), Phys. Lett. B **223**, 485 (1989).
[24] A. C. Benvenuti *et al.* (BCDMS Collaboration), Phys. Lett. B **237**, 592 (1990).
[25] M. Arneodo *et al.* (New Muon Collaboration), Nucl. Phys. **B483**, 3 (1997).
[26] J. P. Berge *et al.*, Z. Phys. C **49**, 187 (1991).
[27] U. K. Yang *et al.* (CCFR/NuTeV Collaboration), Phys. Rev. Lett. **86**, 2742 (2001).
[28] W. G. Seligman *et al.*, Phys. Rev. Lett. **79**, 1213 (1997).
[29] D. A. Mason, Ph.D. thesis, University of Oregon, Report No. FERMILAB-THESIS-2006-01, UMI-32-11223.
[30] M. Goncharov *et al.* (NuTeV Collaboration), Phys. Rev. D **64**, 112006 (2001).
[31] A. Aktas *et al.* (H1 Collaboration), Eur. Phys. J. C **40**, 349 (2005).
[32] H. Abramowicz *et al.* (H1 and ZEUS Collaborations), Eur. Phys. J. C **73**, 2311 (2013).
[33] F. Aaron *et al.* (H1 and ZEUS Collaborations), J. High Energy Phys. 01 (2010) 109.
[34] F. Aaron *et al.* (H1 Collaboration), Eur. Phys. J. C **71**, 1579 (2011).
[35] G. Moreno *et al.*, Phys. Rev. D **43**, 2815 (1991).
[36] R. Towell *et al.* (NuSea Collaboration), Phys. Rev. D **64**, 052002 (2001).
[37] J. Webb *et al.* (NuSea Collaboration), arXiv:hep-ex/0302019.
[38] F. Abe *et al.* (CDF Collaboration), Phys. Rev. Lett. **77**, 2616 (1996).
[39] D. Acosta *et al.* (CDF Collaboration), Phys. Rev. D **71**, 051104 (2005).
[40] V. Abazov *et al.* (D0 Collaboration), Phys. Rev. D **77**, 011106 (2008).
[41] R. Aaij *et al.* (LHCb Collaboration), J. High Energy Phys. 06 (2012) 058.
[42] V. Abazov *et al.* (D0 Collaboration), Phys. Lett. B **658**, 112 (2008).
[43] T. A. Aaltonen *et al.* (CDF Collaboration), Phys. Lett. B **692**, 232 (2010).
[44] CMS Collaboration, Phys. Rev. D **90**, 032004 (2014).

[45] CMS Collaboration, Phys. Rev. Lett. **109**, 111806 (2012).
[46] ATLAS Collaboration, Phys. Rev. D **85**, 072004 (2012).
[47] T. Aaltonen *et al.* (CDF Collaboration), Phys. Rev. D **78**, 052006 (2008).
[48] V. Abazov *et al.* (D0 Collaboration), Phys. Rev. Lett. **101**, 062001 (2008).
[49] ATLAS Collaboration, Phys. Rev. D **86**, 014022 (2012).
[50] CMS Collaboration, Phys. Rev. D **87**, 112002 (2013).
[51] J. C. Collins and J. Pumplin, arXiv:hep-ph/0105207.
[52] J. Pumplin, Phys. Rev. D **81**, 074010 (2010).
[53] J. Pumplin, Phys. Rev. D **80**, 034002 (2009).
[54] P. M. Nadolsky and Z. Sullivan, *Proceedings of Snowmass 2001*, eConf C010630, P510 (2001).
[55] F. Abe *et al.* (CDF Collaboration), Phys. Rev. Lett. **74**, 850 (1995).
[56] E. L. Berger, F. Halzen, C. S. Kim, and S. Willenbrock, Phys. Rev. D **40**, 83 (1989); **40**, 3789 (1989).
[57] A. D. Martin, R. G. Roberts, and W. J. Stirling, Mod. Phys. Lett. A **04**, 1135 (1989).
[58] H.-L. Lai, J. Botts, J. Huston, J. G. Morfin, J. F. Owens, J. Qiu, W.-K. Tung, and H. Weerts, Phys. Rev. D **51**, 4763 (1995).
[59] A. D. Martin, W. J. Stirling, and R. G. Roberts, Phys. Rev. D **50**, 6734 (1994).
[60] F. D. Aaron *et al.* (H1 Collaboration), Eur. Phys. J. C **71**, 1769 (2011); **72**, 2252(E) (2012).
[61] A. Aktas *et al.* (H1 Collaboration), Eur. Phys. J. C **45**, 23 (2006).
[62] S. Chekanov *et al.* (ZEUS Collaboration), Phys. Rev. D **69**, 012004 (2004).
[63] J. Breitweg *et al.* (ZEUS Collaboration), Eur. Phys. J. C **12**, 35 (2000).
[64] J. Gao, M. Guzzi, and P. M. Nadolsky, Eur. Phys. J. C **73**, 2541 (2013).
[65] ATLAS Collaboration, Phys. Rev. D **90**, 072004 (2014).
[66] CMS Collaboration, Eur. Phys. J. C **75**, 542 (2015).
[67] CMS Collaboration, Eur. Phys. J. C **73**, 2339 (2013).
[68] A. Mitov, in Proceedings of the 23rd Workshop on Deep Inelastic Scattering and Related Subjects, DIS 2015 (unpublished), https://indico.cern.ch/event/341292/session/3/contribution/257.
[69] J. H. Kühn, A. Scharf, and P. Uwer, Phys. Rev. D **91**, 014020 (2015).
[70] J. H. Kühn, A. Scharf, and P. Uwer, Eur. Phys. J. C **51**, 37 (2007).
[71] C. Anastasiou, L. J. Dixon, K. Melnikov, and F. Petriello, Phys. Rev. Lett. **91**, 182002 (2003).
[72] C. Anastasiou, L. J. Dixon, K. Melnikov, and F. Petriello, Phys. Rev. D **69**, 094008 (2004).
[73] C. Balazs, J. Qiu, and C.-P. Yuan, Phys. Lett. B **355**, 548 (1995).
[74] C. Balazs and C.-P. Yuan, Phys. Rev. D **56**, 5558 (1997).
[75] F. Landry, R. Brock, P. M. Nadolsky, and C.-P. Yuan, Phys. Rev. D **67**, 073016 (2003).
[76] M. Guzzi, P. M. Nadolsky, and B. Wang, Phys. Rev. D **90**, 014030 (2014).
[77] M. C. Kumar and S. O. Moch, Phys. Lett. B **730**, 122 (2014).
[78] N. Kidonakis and J. F. Owens, Phys. Rev. D **63**, 054019 (2001).
[79] R. D. Ball *et al.* (NNPDF Collaboration), J. High Energy Phys. 04 (2015) 040.
[80] J. Gao, Z. Liang, D. E. Soper, H.-L. Lai, P. M. Nadolsky, and C.-P. Yuan, Comput. Phys. Commun. **184**, 1626 (2013).
[81] R. D. Ball *et al.*, J. High Energy Phys. 04 (2013) 125.
[82] M. Cacciari and N. Houdeau, J. High Energy Phys. 09 (2011) 039.
[83] A. Gehrmann-De Ridder, T. Gehrmann, E. W. N. Glover, and J. Pires, Phys. Rev. Lett. **110**, 162003 (2013).
[84] J. Currie, A. Gehrmann-De Ridder, E. W. N. Glover, and J. Pires, J. High Energy Phys. 01 (2014) 110.
[85] S. Carrazza and J. Pires, J. High Energy Phys. 10 (2014) 145.
[86] M. Wobisch *et al.* (fastNLO Collaboration), arXiv:1109.1310.
[87] T. Carli, D. Clements, A. Cooper-Sarkar, C. Gwenlan, G. P. Salam, F. Siegert, P. Starovoitov, and M. Sutton, Eur. Phys. J. C **66**, 503 (2010).
[88] Z. Nagy, Phys. Rev. Lett. **88**, 122003 (2002).
[89] Z. Nagy, Phys. Rev. D **68**, 094002 (2003).
[90] T. Lewis, Australian Journal of statistics **30A**, 160 (1988).
[91] G. D'Agostini, Nucl. Instrum. Methods Phys. Res., Sect. A **346**, 306 (1994).
[92] G. D'Agostini, Report Nos. CERN-99-03 and CERN-YELLOW-99-03.
[93] H.-L. Lai, P. M. Nadolsky, J. Pumplin, D. Stump, W.-K. Tung, and C.-P. Yuan, J. High Energy Phys. 04 (2007) 089.
[94] J. F. Owens, A. Accardi, and W. Melnitchouk, Phys. Rev. D **87**, 094012 (2013).
[95] M. Czakon, P. Fiedler, and A. Mitov, Phys. Rev. Lett. **110**, 252004 (2013).
[96] M. Czackon and A. Mitov, Comput. Phys. Commun. **185**, 2930 (2014).
[97] C. Anastasiou, S. Buehler, F. Herzog, and A. Lazopoulos, J. High Energy Phys. 12 (2011) 058.
[98] CMS Collaboration, Phys. Rev. Lett. **112**, 191802 (2014).
[99] S. D. Ellis, Z. Kunszt, and D. E. Soper, Phys. Rev. Lett. **69**, 1496 (1992).
[100] Z. Kunszt and D. E. Soper, Phys. Rev. D **46**, 192 (1992).
[101] M. Cacciari, G. P. Salam, and G. Soyez, Eur. Phys. J. C **72**, 1896 (2012).
[102] ATLAS Collaboration, Eur. Phys. J. C **73**, 2509 (2013).
[103] A. D. Martin, A. J. T. M. Mathijssen, W. J. Stirling, R. S. Thorne, B. J. A. Watt, and G. Watt, Eur. Phys. J. C **73**, 2318 (2013).
[104] A. Accardi, W. Melnitchouk, J. F. Owens, M. E. Christy, C. E. Keppel, L. Zhu, and J. G. Morfin, Phys. Rev. D **84**, 014008 (2011).
[105] ATLAS Collaboration, Phys. Lett. B **725**, 223 (2013).
[106] ATLAS Collaboration, J. High Energy Phys. 06 (2014) 112.
[107] K. Melnikov and F. Petriello, Phys. Rev. D **74**, 114017 (2006).
[108] R. Gavin, Y. Li, F. Petriello, and S. Quackenbush, Comput. Phys. Commun. **182**, 2388 (2011).
[109] R. Gavin, Y. Li, F. Petriello, and S. Quackenbush, Comput. Phys. Commun. **184**, 208 (2013).

[110] Y. Li and F. Petriello, Phys. Rev. D **86**, 094034 (2012).
[111] ATLAS Collaboration, Phys. Rev. Lett. **109**, 012001 (2012).
[112] ATLAS Collaboration, J. High Energy Phys. 05 (2014) 068.
[113] CMS Collaboration, J. High Energy Phys. 02 (2014) 013.
[114] S. Alekhin *et al.*, Eur. Phys. J. C **75**, 304 (2015).
[115] O. Samoylov *et al.* (NOMAD Collaboration), Nucl. Phys. **B876**, 339 (2013).
[116] S. Alekhin, J. Bluemlein, L. Caminadac, K. Lipka, K. Lohwasser, S. Moch, R. Petti, and R. Placakyte, Phys. Rev. D **91**, 094002 (2015).
[117] J. M. Campbell and R. K. Ellis, Nucl. Phys. B, Proc. Suppl. **205–206**, 10 (2010).
[118] S. Dittmaier *et al.* (LHC Higgs Cross Section Working Group Collaboration), arXiv:1101.0593.
[119] S. Dittmaier *et al.*, arXiv:1201.3084.
[120] S. Heinemeyer *et al.* (LHC Higgs Cross Section Working Group Collaboration), arXiv:1307.1347.
[121] C. Schmidt, S. Dulat, J. Gao, M. Guzzi, T.-J. Hou, J. W. Huston, P. Nadolsky, J. Pumplin, D. Stump, and C.-P. Yuan, *Proc. Sci.*, DIS2014 (2014) 146.
[122] S. Dulat, T.-J. Hou, J. Gao, J. Huston, P. Nadolsky, J. Pumplin, C. Schmidt, and D. Stump, and C.-P. Yuan, Phys. Rev. D **89**, 113002 (2014).
[123] H.-L. Lai, J. Huston, Z. Li, P. Nadolsky, J. Pumplin, D. Stump, and C.-P. Yuan, Phys. Rev. D **82**, 054021 (2010).
[124] L. A. Harland-Lang, A. D. Martin, P. Motylinski, and R. S. Thorne, Eur. Phys. J. C **75**, 204 (2015).
[125] J. M. Campbell, J. W. Huston, and W. J. Stirling, Rep. Prog. Phys. **70**, 89 (2007).
[126] ATLAS Collaboration, Phys. Lett. B **707**, 459 (2012).
[127] ATLAS Collaboration, Phys. Rev. D **91**, 112013 (2015).
[128] CMS Collaboration, J. High Energy Phys. 11 (2012) 067.
[129] CMS Collaboration, Report No. CMS-PAS-TOP-12-006.
[130] CMS Collaboration, Report No. CMS-PAS-TOP-14-016.
[131] ATLAS Collaboration, Reports Nos. ATLAS-CONF-2012-134 and ATLAS-COM-CONF-2012-166.
[132] M. Czakon, M. L. Mangano, A. Mitov, and J. Rojo, J. High Energy Phys. 07 (2013) 167.
[133] M. Guzzi, K. Lipka, and S. O. Moch, J. High Energy Phys. 01 (2015) 082.
[134] CTEQ-TEA group (to be published).
[135] http://hep.pa.msu.edu/cteq/public/ct14.html.
[136] http://hep.pa.msu.edu/cteq/public/ct14/lhapdf/v5/.
[137] S. Brodsky (private communication).
[138] A. D. Martin, W. J. Stirling, R. S. Thorne, and G. Watt, Eur. Phys. J. C **63**, 189 (2009).
[139] H. Abramowicz *et al.* (H1 and ZEUS Collaborations), Eur. Phys. J. C **75**, 580 (2015).
[140] O. Zenaiev *et al.*, Eur. Phys. J. C **75**, 396 (2015).
[141] J. Pumplin, Phys. Rev. D **82**, 114020 (2010).